Simulation of random set models for unions of discs and the use of power tessellations

Møller, Jesper; Helisová, Katerina

Publication date:
2009

Document Version
Publisher's PDF, also known as Version of record

AALBORG UNIVERSITY

Simulation of random set models for unions of discs and the use of power tessellations

by

Jesper Møller and Kateřina Helisová

R-2009-05

April 2009

Department of Mathematical Sciences
Aalborg University
Fredrik Bajers Vej 7 G ▪ DK - 9220 Aalborg Øst ▪ Denmark
Phone: +45 99 40 80 80 ▪ Telefax: +45 98 15 81 29
URL: http://www.math.aau.dk

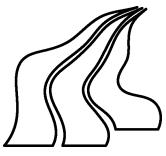

ISSN 1399–2503 ▪ On-line version ISSN 1601–7811

Simulation of random set models for unions of discs and the use of power tessellations

Jesper Møller
Department of Mathematical Sciences
Aalborg University
Aalborg, Denmark
jm@math.aau.dk

Kateřina Helisová
Department of Mathematics
Czech Technical University in Prague
Prague, Czech Republic
helisova@math.feld.cvut.cz

Abstract

The power tessellation (or power diagram or Laguerre diagram) turns out to be particular useful in connection to a certain class of stochastic models for a disc process used for generating a random set model. We discuss how to simulate these models and calculate various characteristics of power tessellations, where some new relations are established. The proposed model is fitted to a heather dataset.

1. Introduction

This paper concerns the simulation of a random set given by a finite union of discs generated by a certain class of stochastic models. In this connection the power tessellation (or power diagram or Laguerre diagram) turns out to be particular useful. As a running example for this paper, Fig. 1 shows a finite configuration of discs, and Fig. 2 shows the power tessellation of the union of these discs. The present paper is based on our previous work [11, 12] but now with a focus on the aspects related to power tessellations. A substantial part of this work has been the developments of codes in `C` and `R` for constructing power tessellations and making simulations of our models. The codes are available at `www.math.aau.dk/~jm/Codes.union.of.discs` and at `www.math.aau.dk/~jm/Codes.likelihood.union.of.discs`.

The paper is organized as follows. Section 2 considers our stochastic models which extend the Boolean model based on a Poisson disc process (the commonly used disc process model) to a more flexible model class with interaction by specifying a probability distribution which depends on certain characteristics of the union of discs such as area, perimeter, and other geometric properties to be specified later. Section 3 provides the details on the power tessellation for a union of discs as needed for subsequent sections. Section 4 considers a birth-death type algorithm for simulation of the disc processes, and Section 5 discusses in detail how successive power tessellations can be constructed when a new disc is added or an existing disc is removed. Section 6 deals with geometric characteristics and inclusion-exclusion formulae for a union of discs and how to make local computations when considering a successive construction of power tessellations as in Sections 4 and 5. The section contains some new results which might be of general interest for readers interested in power diagrams. Section 7 discusses the statistical aspects by considering a particular dataset and a fitted disc process based on our models. Section 8 contains concluding remarks.

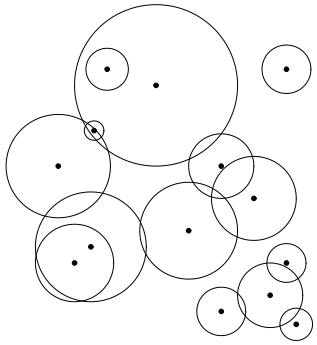

Figure 1. A configuration of discs in general position.

2. Stochastic models

We use the following notation. The d-dimensional Euclidean space is denoted $\mathbb{R}^d$. Let $S \subset \mathbb{R}^2$ be a bounded set defining the region of centres of discs to be considered in the sequel. Identify a two-dimensional closed disc $b(z,r)$ with centre $z \in S$ and radius $r > 0$ by the point $x = (z,r) \in S \times (0,\infty)$. Then, denoting the disc process by $\mathbf{X}$, a

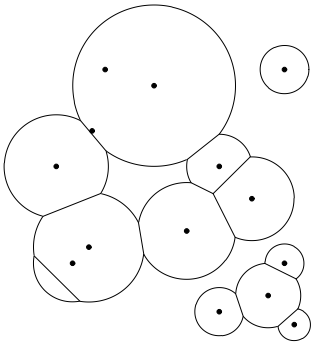

Figure 2. The power tessellation of the union of discs in Fig. 1.

realization of $\mathbf{X}$ can be identified as a finite configuration of such points, i.e. $\mathbf{X} = \{(z_1, r_1), \ldots, (z_n, r_n)\} \subset S \times (0, \infty)$ $(0 \leq n < \infty)$. Moreover, the corresponding realization of the random set, denoted $\mathcal{U}_{\mathbf{X}}$, is $\mathcal{U}_{\mathbf{X}} = \cup_{i=1}^{n} b(z_i, r_i)$. In the special case $n = 0$, we consider $\mathbf{X} = \emptyset$ as the empty configuration and $\mathcal{U}_{\mathbf{X}} = \emptyset$ as the empty subset of $\mathbb{R}^2$.

The commonly used model for the random set is a *Boolean model* [9]. Then the distribution of $\mathbf{X}$ is specified by an intensity function $\rho : S \to [0, \infty)$ for the centres, where $\mu = \int_S \rho(z)\,\mathrm{d}z$ is assumed to be strictly positive and finite, together with a distribution Q on $(0, \infty)$ for the radii. Specifically, the number N of discs specified by $\mathbf{X}$ is then Poisson distributed with mean μ, and conditional on N, the $2N$ random variables given by the centres and radii of the discs are mutually independent, each centre has density $\rho(z)/\mu$ on S, and each radius follows the distribution Q. In other words, $\mathbf{X}$ is a *Poisson process* on $S \times (0, \infty)$ with intensity measure $\mathrm{d}z\,Q(\mathrm{d}r)$, see [9]. Fig. 8 shows a simulation of the Boolean model within a rectangular window $W = [0, 20] \times [0, 10]$, where ρ is equal to the constant 2.45 and Q is the uniform distribution on $[0, 2.45]$.

Since the independence properties of the Poisson process imply a lack of interaction, more interesting models have been introduced in [7] and further generalized in [11] to a class of models called T*-interaction disc processes*. Here T is the six-dimensional statistic

$$T(\mathbf{x}) = (A(\mathcal{U}_{\mathbf{x}}), L(\mathcal{U}_{\mathbf{x}}), \chi(\mathcal{U}_{\mathbf{x}}), N_{\mathrm{h}}(\mathcal{U}_{\mathbf{x}}), N_{\mathrm{ic}}(\mathcal{U}_{\mathbf{x}}), N_{\mathrm{bv}}(\mathcal{U}_{\mathbf{x}})), \tag{1}$$

where A means area, L perimeter, χ Euler-Poincaré characteristic (i.e. the number of connected components minus the number of holes), N_{h} number of holes, N_{ic} number of isolated cells, and N_{bv} number of boundary vertices. Section 6 relates these characteristics to the cells of the power tessellation of $\mathcal{U}_{\mathbf{x}}$. By an isolated cell we mean a disc which is not intersected by another disc in $\mathbf{x}$, and a boundary vertex is the intersection point of two arcs of the boundary of $\mathcal{U}_{\mathbf{x}}$. Moreover, let $\theta = (\theta_1, \ldots, \theta_6) \in \mathbb{R}^6$ denote a six-dimensional parameter vector, and for vectors $t = (t_1, \ldots, t_6) \in \mathbb{R}^6$, define the usual inner product on $\mathbb{R}^6$ by $\theta \cdot t = \sum_{i=1}^{6} \theta_i t_i$. Then the density f_θ of the T-interaction disc process $\mathbf{X}$ with respect to the Poisson process on $S \times (0, \infty)$ with intensity measure $\mathrm{d}z\,Q(\mathrm{d}r)$ is given by

$$f_\theta(\mathbf{x}) = \frac{1}{c_\theta} \exp\left(\theta \cdot T(\mathbf{x})\right), \tag{2}$$

where θ is chosen such that the density is well-defined, i.e. such that

$$c_\theta = \exp\left(\int_{S\times(0,\infty)} \rho(z)\,\mathrm{d}zQ(\mathrm{d}r\right) \times$$
$$\sum_{n=0}^{\infty} \int_{S\times(0,\infty)} \cdots \int_{S\times(0,\infty)} \exp\left(\theta \cdot T(\{(z_1, r_1), \ldots, (z_n, r_n)\})\right)$$
$$\mathrm{d}z_1 Q(\mathrm{d}r_1) \cdots \mathrm{d}z_n Q(\mathrm{d}r_n)$$

is finite (in the sum, if $n = 0$ then the integral is set to one). For a general characterization of the parameter space $\Theta = \{\theta \in \mathbb{R}^6 : c_\theta < \infty\}$ and a discussion on how to handle the intractable normalizing constant c_θ when making simulation-based statistical inference based on Markov chain Monte Carlo methods, see [12, 13]. For instance, if Q has bounded support, then $\Theta = \mathbb{R}^6$ is the entire space. Fig. 9 shows a simulation of the T-interaction process within the region $W = [0, 20] \times [0, 10]$ and with a density with respect to the Poisson process used in Fig. 8 and where $\theta = (-4.91, 1.18, -1.75, -1.75, 0, 0)$ (in this case $\Theta = \mathbb{R}^6$ and further simulations can be found in [12].

The reference Poisson process agrees with the T-interaction disc process if $\theta = 0$. When $\theta \neq 0$, the density $f_\theta(\mathbf{x})$ depends only on $\mathbf{x}$ through $\mathcal{U}_{\mathbf{x}}$, or more precisely only on the geometric characteristics $A(\mathcal{U}_{\mathbf{x}}), \ldots, N_{\mathrm{bv}}(\mathcal{U}_{\mathbf{x}})$. This is advantageous, since in applications often only $\mathcal{U}_{\mathbf{x}}$ may be observable (and possibly only within some window as discussed in Section 7) while $\mathbf{x}$ may be incompletely observed.

3. Power tessellation of a union of discs

This section defines and studies the power tessellation of a union of discs $\mathcal{U} = \cup_{i\in I} b_i$. For specificity we assume that the index set $I = \{1, \ldots, n\}$ is finite, though everything in this section immediately extends to the case where I is countable.

We assume that the discs b_i, $i \in I$ satisfy the general position assumption (henceforth GPA). This means the following. Identify $\mathbb{R}^2$ with the hyperplane of $\mathbb{R}^3$ spanned by

the first two coordinate axes. For each disc $b(z,r)$, define the *ghost sphere* $s(z,r) = \{y \in \mathbb{R}^3 : \|y-z\| = r\}$, i.e. the hypersphere in $\mathbb{R}^3$ with centre z and radius r. A configuration of discs is said to be in *general position* if the intersection of any $k+1$ corresponding ghost spheres is either empty or a sphere of dimension $2-k$, where $k = 1, 2, \ldots$. Note that the intersection is assumed to be empty if $k > 2$, and a sphere of dimension 0 is assumed to consists of two points. Fig. 1 shows a finite configuration of discs in general position. It can be verified that with probability one a realization of any disc process model considered in this paper satisfies the GPA, see [11].

For each disc b_i ($i \in I$) with ghost sphere s_i, let $s_i^+ = \{(y_1,y_2,y_3) \in s_i : y_3 \geq 0\}$ denote the corresponding upper hypersphere, and for $u \in b_i$, let $y_i(u)$ denote the unique point on s_i^+ those orthogonal projection on $\mathbb{R}^2$ is u. The subset of s_i^+ consisting of those points "we can see from above" is given by

$$C_i = \{y_i(u) : u \in b_i,\ \|u - y_i(u)\| \geq \|u - y_j(u)\| \text{ whenever } u \in b_j,\ j \in I\},$$

and the GPA implies that the non-empty C_i have disjoint 2-dimensional relative interiors. Thus, as illustrated in Fig. 3, the non-empty C_i form a tessellation (i.e. subdivision) of $\cup_I s_i^+$ corresponding to the 2-dimensional pieces of upper ghost spheres "as seen from above". Projecting this tessellation onto $\mathbb{R}^2$, we obtain a tessellation of $\mathcal{U}$, see Fig. 2. Below we study this tessellation in some detail.

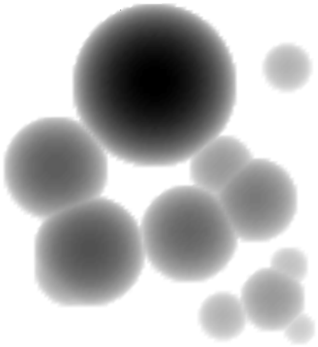

Figure 3. The upper hemispheres as seen from above; the underlying discs are shown in Fig. 1.

Let $J = \{i \in I : C_i \neq \emptyset\}$. For $i \in I$, define the *power distance* of a point $u \in \mathbb{R}^2$ from $b_i = b(z_i, r_i)$ by $\pi_i(u) = \|u - z_i\|^2 - r_i^2$, and define the *power cell* associated with b_i by

$$V_i = \{u \in \mathbb{R}^2 : \pi_i(u) \leq \pi_j(u) \text{ for all } j \in I\}.$$

For distinct $i, j \in I$, define the closed halfplane $H_{i,j} = \{u \in \mathbb{R}^2 : \pi_i(u) \leq \pi_j(u)\}$. Each V_i is a convex polygon, since it is a finite intersection of closed halfplanes $H_{i,j}$. The power cells have disjoint interiors, and by GPA, each V_i is either empty or of dimension two. Consequently, the non-empty power cells V_i, $i \in J$ constitute a tessellation of $\mathbb{R}^2$ called the *power diagram* (or *Laguerre diagram*), see [1] and the references therein. In the special case where all radii r_i are equal, we have $I = J$ and the power diagram is a Voronoi tessellation (e.g. [10, 14]) where each cell V_i contains z_i in its interior. If the radii are not equal, a power cell V_i may not contain z_i, since $H_{i,j}$ may not contain z_i.

Let B_i denote the orthogonal projection of C_i on $\mathbb{R}^2$. By Pythagoras, for all $u \in b_i$, $\pi_i(u) + \|u - y_i(u)\|^2 = 0$. Consequently, for any $i, j \in I$ and $u \in b_i \cap b_j$,

$$\|u - y_i(u)\| \geq \|u - y_j(u)\| \quad \text{if and only if} \quad \pi_i(u) \leq \pi_j(u).$$

Thus $B_i = V_i \cap b_i$. By GPA and the one-to-one correspondence between B_i and C_i, the collection of sets B_i, $i \in J$ constitutes a subdivision of $\mathcal{U}$ into 2-dimensional convex sets with disjoint interiors. We call this the *power tessellation of the union of discs* and denote it by $\mathcal{B}$. Further, if $i \in J$, we call B_i the *power cell restricted to its associated disc* b_i (clearly, $B_i = \emptyset$ if $i \in I \setminus J$). Since V_i may not contain z_i, B_i may not contain z_i; an example of this is shown in Fig. 2. We say that a cell B_i is *isolated* if $B_i = b_i$.

It is illuminating to consider Figure 2 when making the following definitions. If the intersection $e_{i,j} = B_i \cap B_j$ between two cells of $\mathcal{B}$ is non-empty, then $e_{i,j} = [u_{i,j}, v_{i,j}]$ is a closed line segment, where $u_{i,j}$ and $v_{i,j}$ denote the endpoints, and we call $e_{i,j}$ an *interior edge* of $\mathcal{B}$. The vertices of $\mathcal{B}$ are given by all endpoints of interior edges. A vertex of $\mathcal{B}$ lying on the boundary $\partial\mathcal{U}$ is called a *boundary vertex*, and it is called an *interior vertex* otherwise. Each circular arc on $\mathcal{B}$ defined by two successive boundary vertices is called a *boundary edge* of $\mathcal{B}$. The circle given by the boundary of an isolated cell of $\mathcal{B}$ is also called a boundary edge or sometimes an *isolated boundary edge*. The connected components of $\partial\mathcal{U}$ are closed curves, and each such curve is a union of certain boundary edges which either bound a hole, in which case the curve is called an *inner boundary curve*, or bound a connected component of $\mathcal{U}$, in which case the curve is called an *outer boundary curve*. A generic boundary edge of $\mathcal{B}$ is written as $\lfloor u_i, v_i \rceil$ if $B_i \neq b_i$ (a non-isolated cell), where the index means that u_i and v_i are boundary vertices of B_i, or as ∂b_i if $B_i = b_i$. We order u_i and v_i such that $\lfloor u_i, v_i \rceil$ is the circular arc from u_i to v_i when ∂b_i is considered anti-clockwise.

By GPA, any intersection among four cells of $\mathcal{B}$ is empty, each interior vertex corresponds to a non-empty intersection among three cells of $\mathcal{B}$, and exactly three edges emerge at

each vertex. Note that each isolated cell has no vertices and one edge. Each interior edge $e_{i,j}$ is contained in the *bisector (or power line or radical axis)* of b_i and b_j defined by $\partial H_{i,j} = \{u \in \mathbb{R}^d : \pi_i(u) = \pi_j(u)\}$. This is the line perpendicular to the line joining the centres of the two discs, and passing through the point

$$z_{i,j} = \frac{1}{2}\left(z_i + z_j + \frac{r_j^2 - r_i^2}{\|z_i - z_j\|^2}(z_i - z_j)\right).$$

We call $E_{i,j} \equiv \partial H_{i,j} \cap b_i = \partial H_{i,j} \cap b_j$ the *chord* of $b_i \cap b_j$. Obviously, $e_{i,j} \subseteq E_{i,j}$.

The *dual graph* $\mathcal{D}$ to $\mathcal{B}$ has nodes equal to the centres z_i, $i \in J$ of discs generating non-empty cells, and each edge of $\mathcal{D}$ is given by two vertices z_i and z_j such that $e_{i,j} \neq \emptyset$. See Fig. 4. Note that there is a one-to-one correspondence between the edges of $\mathcal{D}$ and the interior edges of $\mathcal{B}$.

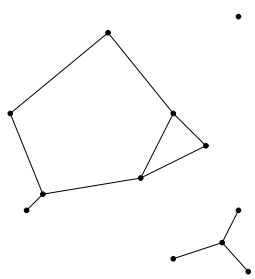

Figure 4. The dual graph corresponding to the power tessellation in Fig. 2.

4. Algorithms for simulation of the disc processes

We can construct the power tessellation of a finite union of discs by successively adding the discs one by one, keeping track on old and new edges and whether each disc generates a non-empty cell or not. This successive construction is considered in Section 5 and is much in line with a Metropolis-Hastings algorithm to be discussed below for the simulation of the T-interaction disc process introduced in Section 2.

4.1. The conditional intensity

The so-called *Papangelou conditional intensity* will play a key role. For a finite configuration $\mathbf{x} = \{(z_1, r_1), \ldots, (z_n, r_n)\}$ specifying $n \in \{0, 1, \ldots\}$ discs with centres in the bounded region S, and for $v = (z, r)$ specifying another disc $b(z, r)$ with centre in S, the Papangelou conditional intensity is defined by

$$\lambda_\theta(\mathbf{x}, v) = f_\theta(\mathbf{x} \cup \{v\})/f_\theta(\mathbf{x}). \tag{3}$$

. Combining (1)-(3), we obtain

$$\lambda_\theta(\mathbf{x}, v) = \exp\big(\theta_1 A(\mathbf{x}, v) + \theta_2 L(\mathbf{x}, v) + \theta_3 \chi(\mathbf{x}, v) + \theta_4 N_{\mathrm{h}}(\mathbf{x}, v) + \theta_5 N_{\mathrm{ic}}(\mathbf{x}, v) + \theta_6 N_{\mathrm{bv}}(\mathbf{x}, v)\big) \tag{4}$$

where for functionals $W = A, L, \ldots$, we define $W(\mathbf{x}, v) = W(\mathcal{U}_{\mathbf{x}\cup\{v\}}) - W(\mathcal{U}_{\mathbf{x}})$. We can interpret $\lambda_\theta(\mathbf{x}, v)\rho(z)\,\mathrm{d}z\,Q(\mathrm{d}r)$ as the conditional probability for observing a disc with centre in an infinitesimally small region around z of area $\mathrm{d}z$ and radius in an infinitesimally small interval around r of length $\mathrm{d}r$, given that the remaining discs of the process are specified by $\mathbf{x}$.

Note that the model is specified by λ_θ, since there is a one-to-one correspondence between f_θ and λ_θ. Moreover, in contrast to f_θ, λ_θ does not depend on the intractable normalizing constant c_θ in (2). Moreover, $\lambda_\theta(\mathbf{x}, v)$ depends only on local information in the sense that it only depends on v and those connected components of $\mathcal{U}_{\mathbf{x}}$ which are intersected by $b(v)$. This is utilized when making simulations as discussed in Sections 4.2 and 6.2.

4.2. Birth-death Metropolis-Hastings algorithm

Simulation of the reference Poisson process with intensity measure $\rho(z)\,\mathrm{d}z\,Q(\mathrm{d}r)$ is straightforward using the definition of this process, see Section 2 and [13]. It is more complicated to simulate a T-interaction disc process with Papangelou conditional intensity (4). In fact other models with $\lambda_\theta(\mathbf{x}, v)$ depending only on $W(\mathbf{x}, v)$ for $W = A, L, \chi, N_{\mathrm{h}}, N_{\mathrm{ic}}, N_{\mathrm{bv}}$ or other characteristics of the power tessellation may also be simulated by the following algorithm.

We use a simple version of the birth-death type Metropolis-Hastings algorithm studied in [5, 6, 13] to generate a Markov chain $\mathbf{X}_t$, $t = 0, 1, \ldots$ which converges towards the T-interaction disc process. The details are given below, where a birth is an addition of a disc and a death is a deletion of an existing disc.

Suppose $\mathbf{X}_t = \mathbf{x}$ is the state at iteration t. Then we generate a proposal which is either a 'birth' $\mathbf{x} \cup \{v\}$ of a new discs $v = (z, r)$ or a 'death' $\mathbf{x} \setminus \{x_i\}$ of an old disc $x_i \in \mathbf{x}$. Each kind of proposal may happen with equal probability

$1/2$. Define

$$r_\theta(\mathbf{x}, v) = \lambda_\theta(\mathbf{x}, v) \frac{\int_S \rho(s)\,\mathrm{d}s}{\rho(z)(n(\mathbf{x})+1)}.$$

In case of a birth-proposal, z has a density on S proportional to ρ, and r follows the distribution Q. This proposal is accepted as the state at iteration $t+1$ with probability $\min\{1, H_\theta(\mathbf{x}, v)\}$, where the Hastings ratio is given by $H_\theta(\mathbf{x}, v) = r_\theta(\mathbf{x}, v)$. In case of a death-proposal, x_i is a uniformly selected point from $\mathbf{x}$, and the Hastings ratio in the acceptance probability of the proposal is now given by $H_\theta(\mathbf{x}, x_i) = 1/r_\theta(\mathbf{x} \setminus \{x_i\}, x_i)$ (in the special case where $\mathbf{x} = \emptyset$, we do nothing). Finally, if neither kind of proposal is accepted, we retain $\mathbf{x}$ at iteration $t+1$.

As verified in [6], the generated Markov chain is aperiodic and positive Harris recurrent, the chain converges towards the distribution of $\mathbf{X}$, and Birkhoff's ergodic theorem establishes convergence of Monte Carlo estimates of mean values with respect to T-interaction process (2). In some cases local stability is satisfied, meaning that for some constant K_θ we have

$$\lambda_\theta(\mathbf{x}, v) \leq K_\theta; \tag{5}$$

see Proposition 7 in [11]. Then the chain is geometrical ergodic, and hence a central limit theorem applies for Monte Carlo estimates, see [2, 13, 15]. Moreover, from a computational perspective, the important point of the algorithm is that it only involves calculating the Papangelou conditional intensity, so only local computations of the statistics appearing in (4) are needed.

Denote the support of Q by $\mathrm{supp}(Q)$, and the support of the intensity measure of the reference Poisson process by

$$\Omega = \{(z, r) \in S \times (0, \infty) : \rho(z) > 0, r \in \mathrm{supp}(Q)\}.$$

Let $\mathcal{N}$ be the set of all finite configurations $\mathbf{x} \in \Omega$ so that the discs given by $\mathbf{x}$ are in general position. In theory we may use any state of $\mathcal{N}$ as the initial state of the algorithm, but we have mainly used three kinds of initial states:

(a) the extreme case of the empty configuration $\emptyset$;
(b) if local stability is satisfied, the other extreme case is given by a realization from a Poisson process D with intensity measure $K_\theta \rho(z)\,\mathrm{d}z\, Q(\mathrm{d}r)$, where K_θ is the upper bound in (5);
(c) a realization of the reference Poisson disc process Ψ with intensity measure $\mathrm{d}z\, Q(\mathrm{d}r)$ (an intermediate case of (a)-(b) if $K_\theta > 1$).

When local stability is satisfied, there exists a coupling between the T-interaction process X and the Poisson processes D and Ψ in (b) and (c) such that D dominates both X and Ψ, i.e. $X \subseteq D$ and $\Psi \subseteq D$. See [8].

5. Successive construction of power tessellations

This section explains how to construct a new power tessellation of a union of discs by adding a new ball (Section 5.1) or deleting an old ball (Section 5.2), assuming that the old power tessellation is known. This is exactly what is needed for the birth-death Metropolis-Hastings algorithm in Section 4.2. The constructions can easily be extended to keep track on the connected components of the union of discs, but to save space we omit those details.

5.1. The case where a new disc is added

Suppose we want to construct a new power tessellation $\mathcal{B}^{\mathrm{new}}$ of a union $\mathcal{U}^{\mathrm{new}} = \cup_1^n b_i$ of $n \geq 1$ discs in general position, where we are adding the disc b_n and we have already constructed the power tessellation $\mathcal{B}^{\mathrm{old}}$ of $\mathcal{U}^{\mathrm{old}} = \cup_1^{n-1} b_i$ based on the $n-1$ other discs (if $n = 1$ then $\mathcal{B}^{\mathrm{old}}$ and $\mathcal{U}^{\mathrm{old}}$ are empty). More precisely, with respect to $\mathcal{B}^{\mathrm{old}}$, we assume to know all the old edges. We denote old interior edges by $[u_{i,j}^{\mathrm{old}}, v_{i,j}^{\mathrm{old}}]$ and old boundary edges by $\rfloor u_i^{\mathrm{old}}, v_i^{\mathrm{old}} \lceil$ or $\partial b_i^{\mathrm{old}}$. We want to construct the new tessellation $\mathcal{B}^{\mathrm{new}}$ of $\mathcal{U}^{\mathrm{new}} = \mathcal{U}^{\mathrm{old}} \cup b_n$ by finding its interior edges $[u_{i,n}^{\mathrm{new}}, v_{i,n}^{\mathrm{new}}]$ and boundary edges $\rfloor u_n^{\mathrm{new}}, v_n^{\mathrm{new}} \lceil$ associated to the new cell B_n^{new}. This is done in steps (ii) and (iv) below. Moreover, to obtain the remaining new edges, we modify old interior edges $[u_{i,j}^{\mathrm{old}}, v_{i,j}^{\mathrm{old}}]$ and old boundary edges $\rfloor u_i^{\mathrm{old}}, v_i^{\mathrm{old}} \lceil$ or $\partial b_i^{\mathrm{old}}$, noticing that a "modified old edge" can be unchanged, reduced or disappearing. This is done in steps (iii) and (v) below. Notice that steps (i), (ii), and (iv) determine the new cells, i.e. which of the sets $B_1^{\mathrm{new}}, \ldots, B_n^{\mathrm{new}}$ are empty or not.

(i) Considering old discs intersecting the new disc: If b_n is contained in some disc b_j with $j < n$, then B_n^{new} is empty and so $\mathcal{B}^{\mathrm{new}} = \mathcal{B}^{\mathrm{old}}$ is unchanged. Assume that b_n is not contained in any disc b_j with $j < n$, and without loss of generality that b_n intersects $B_1^{\mathrm{old}}, \ldots, B_i^{\mathrm{old}}$ but not $B_{i+1}^{\mathrm{old}}, \ldots, B_{n-1}^{\mathrm{old}}$, where $0 \leq i \leq n-1$ (setting $i = 0$ if b_n has no intersection). Then $B_j^{\mathrm{new}} = B_j^{\mathrm{old}}$ is unchanged for $j = i+1, \ldots, n-1$, so it suffices below to find the edges of $B_1^{\mathrm{new}}, \ldots, B_i^{\mathrm{new}}$ and B_n^{new}.

If $i = 0$ then $B_n^{\mathrm{new}} = b_n$ is an isolated cell with boundary edge ∂b_n. In (ii)-(v) we assume that $i \geq 1$.

(ii) Finding the interior edges of B_n^{new}: To obtain the interior edges of B_n^{new}, for $j = 1, \ldots, i$, we start by assigning $e_{j,n}^{\mathrm{new}} \leftarrow [u_{j,n}^{\mathrm{new}}, v_{j,n}^{\mathrm{new}}]$, considering $u_{j,n}^{\mathrm{new}}$ and $v_{j,n}^{\mathrm{new}}$ as (potential) boundary vertices given by the endpoints of the chord $E_{j,n}$. Further, for $k = 1, \ldots, i$ with $k \neq j$, if $e_{j,n}^{\mathrm{new}} \cap H_{n,k} = \emptyset$ (or equivalently $u_{j,n}^{\mathrm{new}} \notin H_{n,k}$ and $v_{j,n}^{\mathrm{new}} \notin H_{n,k}$, since $H_{n,k}$ is convex) we obtain that $e_{j,n}^{\mathrm{new}} \leftarrow \emptyset$ and we can stop the k-loop, else $e_{j,n}^{\mathrm{new}} \leftarrow e_{j,n}^{\mathrm{new}} \cap H_{n,k}$. In the latter case, either both vertices are contained in $H_{n,k}$ and so the edge remains unchanged, or exactly one vertex is

not contained in $H_{n,k}$, e.g. $u_{j,n}^{\rm new} \notin H_{n,k}$ but $v_{j,n}^{\rm new} \in H_{n,k}$, in which case $u_{j,n}^{\rm new}$ becomes an interior vertex given by the point $e_{j,n}^{\rm new} \cap \partial H_{n,k}$ while $v_{j,n}^{\rm new}$ is unchanged. In this way we find all interior edges of $B_n^{\rm new}$, and all interior and boundary vertices of $B_n^{\rm new}$.

Since we have assumed that $i > 0$, $B_n^{\rm new}$ is empty if and only if it has no interior edges.

(iii) Modifying the old interior edges: At the same time as we do step (ii) above, we also check whether each interior edge $e_{j,k}^{\rm old} = [u_{j,k}^{\rm old}, v_{j,k}^{\rm old}]$ of $\mathcal{B}^{\rm old}$ with $j < k \leq i$ should be kept, reduced or omitted when we consider $\mathcal{B}^{\rm new}$ (recalling that $e_{j,k}^{\rm new} = e_{j,k}^{\rm old}$ is unchanged if $j > i$ or $k > i$). We have

$$e_{j,k}^{\rm new} = e_{j,k}^{\rm old} \cap H_{j,n} = e_{j,k}^{\rm old} \cap H_{k,n}.$$

Thus $e_{j,k}^{\rm new}$ is empty if $u_{j,k}^{\rm old} \notin H_{k,n}$ and $v_{j,k}^{\rm old} \notin H_{k,n}$, while $e_{j,k}^{\rm new} = e_{j,k}^{\rm old}$ if $u_{j,k}^{\rm old} \in H_{k,n}$ and $v_{j,k}^{\rm old} \in H_{k,n}$. Further, if $u_{j,k}^{\rm old} \in H_{k,n}$ and $v_{j,k}^{\rm old} \notin H_{k,n}$, then $e_{j,k}^{\rm new} = [u_{j,k}^{\rm old}, v_{j,k}^{\rm new}]$ where $v_{j,k}^{\rm new}$ is the point given by $e_{j,k}^{\rm old} \cap \partial H_{k,n}$. Similarly, if $u_{j,k}^{\rm old} \notin H_{k,n}$ and $v_{j,k}^{\rm old} \in H_{k,n}$, then $e_{j,k}^{\rm new} = [u_{j,k}^{\rm new}, v_{j,k}^{\rm old}]$ where $u_{j,k}^{\rm new}$ is the point given by $e_{j,k}^{\rm old} \cap \partial H_{k,n}$.

Note that for each $j \leq i$, $B_j^{\rm new}$ is empty if and only if it has no interior edge.

(iv) Finding the boundary edges of $B_n^{\rm new}$: Suppose that $B_n^{\rm new}$ has $m > 0$ boundary vertices $w_1^{\rm new}, \dots, w_m^{\rm new}$. Notice that m is an even number, and we can organize the boundary vertices such that $w_1^{\rm new} = z_n + r_n(\cos\varphi_1^{\rm new}, \sin\varphi_1^{\rm new})$, …, $w_m^{\rm new} = z_n + r_n(\cos\varphi_m^{\rm new}, \sin\varphi_m^{\rm new})$, where $0 \leq \varphi_1^{\rm new} < \cdots < \varphi_m^{\rm new} < 2\pi$. Then $B_n^{\rm new}$ has $m/2$ boundary edges, namely

$$\lfloor w_2^{\rm new}, w_3^{\rm new} \rceil, \lfloor w_4^{\rm new}, w_5^{\rm new} \rceil, \dots, \lfloor w_m^{\rm new}, w_1^{\rm new} \rceil$$

if $z_n + (r_n, 0) \in H_{n,j}$ for all $j = 1, \dots, i$, and

$$\lfloor w_1^{\rm new}, w_2^{\rm new} \rceil, \lfloor w_3^{\rm new}, w_4^{\rm new} \rceil, \dots, \lfloor w_{m-1}^{\rm new}, w_m^{\rm new} \rceil$$

otherwise.

(v) Modifying the old boundary edges: Finally, we modify the boundary edges $\lfloor u_j^{\rm old}, v_j^{\rm old} \rceil$ of $\mathcal{B}^{\rm old}$ considering $\mathcal{B}^{\rm new}$ and $j \leq i$ (noticing that $\lfloor u_j^{\rm old}, v_j^{\rm old} \rceil$ is a boundary edge of $\mathcal{B}^{\rm new}$ too if $j > i$). This is done in a similar way as in step (iv). Suppose that $B_j^{\rm new}$ has $m_j > 0$ boundary vertices $w_1^{\rm new}, \dots, w_{m_j}^{\rm new}$, which we organize as in (iv). Then $B_j^{\rm new}$ has boundary edges

$$\lfloor w_2^{\rm new}, w_3^{\rm new} \rceil, \lfloor w_4^{\rm new}, w_5^{\rm new} \rceil, \dots, \lfloor w_{m_j}^{\rm new}, w_1^{\rm new} \rceil$$

if $z_j + (r_j, 0) \in H_{j,k}$ for all $k \leq n$ with $k \neq j$ and $b_j \cap b_k \neq \emptyset$, and

$$\lfloor w_1^{\rm new}, w_2^{\rm new} \rceil, \lfloor w_3^{\rm new}, w_4^{\rm new} \rceil, \dots, \lfloor w_{m_j-1}^{\rm new}, w_{m_j}^{\rm new} \rceil$$

otherwise.

5.2. The case where a disc is deleted

Suppose we are deleting the disc b_n from a configuration $\{b_1, \dots, b_n\}$ of $n \geq 1$ discs, which are assumed to be in general position. We also assume that we know the power tessellation $\mathcal{B}^{\rm old}$ of $\mathcal{U}^{\rm old} = \cup_1^n b_i$. Below we explain how to construct the new power tessellation $\mathcal{B}^{\rm new}$ of $\mathcal{U}^{\rm new} = \cup_1^{n-1} b_i$. More precisely, with respect to $\mathcal{B}^{\rm old}$, we assume to know all the interior edges $[u_{i,j}^{\rm old}, v_{i,j}^{\rm old}]$ and all the boundary edges $\lfloor u_i^{\rm old}, v_i^{\rm old} \rceil$. We want to construct the tessellation $\mathcal{B}^{\rm new}$ of $\mathcal{U}^{\rm new} = \mathcal{U}^{\rm old} \setminus b_n$ by finding the interior edges $[u_{i,j}^{\rm new}, v_{i,j}^{\rm new}]$ and the boundary edges $\lfloor u_i^{\rm new}, v_i^{\rm new} \rceil$ associated to each new cell $B_i^{\rm new}$, noticing that $B_i^{\rm new}$ either agrees with $B_i^{\rm old}$ or is an enlargement of $B_i^{\rm old}$ or is a completely new cell. One possibility could be to "reverse" the construction in Section 5.1, where a new disc is added, however, we realized that it is easier to create the new edges without reversing the construction in Section 5.1 but using a construction as described below. This is partly explained by the fact that an old empty set $B_i^{\rm old}$ may possibly be replaced by a non-empty set $B_i^{\rm new}$.

(i) Considering the discs intersecting the disc which is deleted: Clearly, if $B_n^{\rm old}$ is empty, then $\mathcal{B}^{\rm new} = \mathcal{B}^{\rm old}$ is unchanged. Assume that $B_n^{\rm old}$ is a non-empty cell, and without loss of generality that b_n intersects $b_1, \dots, b_i$ but not $b_{i+1}, \dots, b_{n-1}$, where $0 \leq i \leq n-1$ (setting $i = 0$ if b_n has no intersection). Then it suffices to find the edges of $B_1^{\rm new}, \dots, B_i^{\rm new}$, since $B_j^{\rm new} = B_j^{\rm old}$ is unchanged for $j = i+1, \dots, n-1$. If $i = 0$ then $B_n^{\rm old} = b_n$ is an isolated cell, and so $B_1^{\rm new} = B_1^{\rm old}, \dots, B_{n-1}^{\rm new} = B_{n-1}^{\rm old}$ are unchanged. In the following steps (ii)-(iv), suppose that $i > 0$.

(ii) Finding the new interior edges: If $i = 1$, no new interior edge appears. Suppose that $i \geq 2$. We want to determine each set $e_{j,k}^{\rm new}$ with $j < k \leq i$. We start by assigning all cells $B_1^{\rm new}, \dots, B_i^{\rm new}$ to be non-empty, and by assigning $e_{j,k}^{\rm new} \leftarrow [u_{j,k}^{\rm new}, v_{j,k}^{\rm new}]$, considering $u_{j,k}^{\rm new}$ and $v_{j,k}^{\rm new}$ as (potential) boundary vertices given by the endpoints of the chord $E_{j,k}$. Consider a loop with $l = 1, \dots, i$ and $l \neq j, k$. If $e_{j,k}^{\rm new} \cap H_{k,l} = \emptyset$ (or equivalently $u_{j,k}^{\rm new} \notin H_{k,l}$ and $v_{j,k}^{\rm new} \notin H_{k,l}$, since $H_{k,l}$ is convex), we have that $e_{j,k}^{\rm new}$ is empty and we can stop the l-loop. Otherwise assign $e_{j,k}^{\rm new} \leftarrow e_{j,k}^{\rm new} \cap H_{k,l}$, where we notice that only the following two cases can occur. First, if both vertices of $e_{j,k}^{\rm new}$ are contained in $H_{k,l}$, the edge remains unchanged. Second, if exactly one vertex is not contained in $H_{k,l}$, e.g. $u_{j,k}^{\rm new} \notin H_{k,l}$ but $v_{j,k}^{\rm new} \in H_{k,l}$, then $u_{j,k}^{\rm new}$ becomes an interior vertex given by the point $e_{j,k}^{\rm new} \cap \partial H_{k,l}$ while $v_{j,k}^{\rm new}$ is unchanged. When the loop is finished, we have determined all the new interior edges, including the information whether their endpoints are interior or boundary vertices.

(iii) Determining the new cells: For each $j \leq i$, we determine if $B_j^{\rm new}$ is a new cell by checking if it has an edge. Suppose that $B_j^{\rm new}$ has no interior edge, i.e. it is either an

empty set or a new isolated cell. If an arbitrary fixed point of b_j is included in $H_{j,l}$ for all $l = 1, \dots, n-1$ with $l \neq j$, then B_j has exactly one boundary edge and it is an isolated cell. Otherwise B_j^{new} is empty. In this way we determine whether each B_j^{new} is empty or a new cell, including whether it is an isolated cell.

(iv) Finding the new boundary edges: We have already determined the new isolated boundary edges in step (iii). Consider a non-isolated cell B_j^{new} with $j \leq i$ with boundary vertices $w_k^{\mathrm{new}} = z_j + r_j(\cos\varphi_k^{\mathrm{new}}, \sin\varphi_k^{\mathrm{new}})$, $k = 1, \dots, m_j$. Recall that $m_j > 0$ is an even number and we organize the vertices so that $0 \leq \varphi_1^{\mathrm{new}} < \cdots < \varphi_{m_j}^{\mathrm{new}} < 2\pi$, cf. (iv) in Section 5.1. Then B_j^{new} has $m_j/2$ boundary edges, namely

$$\lfloor w_2^{\mathrm{new}}, w_3^{\mathrm{new}} \rceil, \lfloor w_4^{\mathrm{new}}, w_5^{\mathrm{new}} \rceil, \dots, \lfloor w_{m_j}^{\mathrm{new}}, w_1^{\mathrm{new}} \rceil$$

if $z_j + (r_j, 0) \in H_{j,l}$ for all $l = 1, \dots, i$, and

$$\lfloor w_1^{\mathrm{new}}, w_2^{\mathrm{new}} \rceil, \lfloor w_3^{\mathrm{new}}, w_4^{\mathrm{new}} \rceil, \dots, \lfloor w_{m_j-1}^{\mathrm{new}}, w_{m_j}^{\mathrm{new}} \rceil$$

otherwise.

6. Calculation of characteristics of power tessellations and unions of discs

6.1. Geometric characteristics and inclusion-exclusion formulae

Propositions 1-2 below concern various useful relations between certain geometric characteristics of the union of discs $\mathcal{U} = \mathcal{U}_{\mathbf{x}}$ and of its power tessellation $\mathcal{B} = \mathcal{B}_{\mathbf{x}}$, assuming $\mathbf{x} \in \mathcal{N}$. Among other things, the results become useful in connection to verifying Ruelle stability (see [11]), for computation of geometric characteristics in Section 6.2, and for the sequential construction of power tessellations considered in Section 4.2.

Define the number of connected components $N_{\mathrm{cc}} = N_{\mathrm{cc}}(\mathcal{U})$, and the following characteristics of $\mathcal{B}$: the number of non-empty cells $N_{\mathrm{c}} = N_{\mathrm{c}}(\mathcal{B})$, the number of interior edges $N_{\mathrm{ie}} = N_{\mathrm{ie}}(\mathcal{B})$, the number of edges $N_{\mathrm{e}} = N_{\mathrm{be}} + N_{\mathrm{ie}}$, the number of interior vertices $N_{\mathrm{iv}} = N_{\mathrm{iv}}(\mathcal{B})$, and the number of vertices $N_{\mathrm{v}} = N_{\mathrm{bv}} + N_{\mathrm{iv}}$. These statistics do not appear in the T-interaction process specified by (1)-(2) since they cannot be determined from $\mathcal{U}$ but only from $\mathcal{B}$, which usually in practice only $\mathcal{U}$ is observable (and possibly only within some window as discussed in Section 7). Furthermore, let $N = n(\mathbf{x})$ denote the number of discs.

Proposition 1. We have

$$N_{\mathrm{ic}} \leq N_{\mathrm{cc}} \leq N_{\mathrm{c}} \leq N, \quad N_{\mathrm{bv}} = 2N_{\mathrm{ie}} - 3N_{\mathrm{iv}}, \tag{6}$$

and

$$\chi = N_{\mathrm{cc}} - N_{\mathrm{h}} = N_{\mathrm{c}} - N_{\mathrm{ie}} + N_{\mathrm{iv}}. \tag{7}$$

If $N_{\mathrm{c}} \geq 2$ and $N_{\mathrm{cc}} = 1$, then

$$N_{\mathrm{be}} = N_{\mathrm{bv}} \leq 2N_{\mathrm{ie}}, \quad 3N_{\mathrm{v}} = 2N_{\mathrm{e}}. \tag{8}$$

If $N_{\mathrm{c}} \geq 3$ and $N_{\mathrm{cc}} = 1$, then

$$N_{\mathrm{ie}} \leq 3N_{\mathrm{c}} - 6. \tag{9}$$

Moreover,

$$N_{\mathrm{bv}} \leq 6N \tag{10}$$

and

$$N_{\mathrm{h}} = 0 \quad \text{if } N_{\mathrm{c}} \leq 2, \qquad N_{\mathrm{h}} \leq 2N_{\mathrm{c}} - 5 \quad \text{if } N_{\mathrm{c}} \geq 3. \tag{11}$$

Proof. The inequalities in (6) clearly hold, and the identity in (6) follows from a simple counting argument, using that each interior edge has two endpoints, and exactly three interior edges emerge at each interior vertex.

The first identity in (7) is just the definition of χ (see Section 2) and the second identity follows from Euler's formula.

Assuming $N_{\mathrm{c}} \geq 2$ and $N_{\mathrm{cc}} = 1$, (8) follows from simple counting arguments, using first that exactly two boundary edges emerge at each boundary vertex, second the simple fact that $N_{\mathrm{bv}} \leq N_{\mathrm{v}}$, and third that exactly three edges emerge at each vertex.

To verify (9), consider the dual graph $\mathcal{D}$. Since we assume that $N_{\mathrm{c}} \geq 3$ and $N_{\mathrm{cc}} = 1$, $\mathcal{D}$ has N_{ie} edges and N_{c} vertices, and so by planar graph theory [16], since $\mathcal{D}$ is a connected graph without multiple edges, the number of dual edges is bounded by $3N_{\mathrm{c}} - 6$.

To verify (10), note that $N_{\mathrm{bv}} \leq 2N_{\mathrm{ie}}$, cf. (6). Using (9) and considering a sum over all components, we obtain that N_{ie} is bounded above by the number of components with two cells plus three times the number of components with three or more cells. Consequently, $N_{\mathrm{bv}} \leq 6N$.

Finally, to verify (11), note that N_{h} is given by the sum of number of holes of all connected components of $\mathcal{U}$, and a connected component consisting of one or two power cells has no holes, so it suffices to consider the case where $N_{\mathrm{cc}} = 1$ and $N_{\mathrm{c}} \geq 3$. Then by (7), N_{h} is bounded above by $1 - (N_{\mathrm{c}} - N_{\mathrm{ie}})$, which in turn by (9) is bounded above by $2N_{\mathrm{c}} - 5$.

Equation (11) is a main result in [7]. Our proof of (11) is much simpler and shorter, demonstrating the usefulness of the power tessellation and its dual graph. The upper bound in (11) can be obtained for any three or more discs: If $\mathbf{x}$ consists of three discs b_1, b_2, b_3 such that $b_i \cap b_j \neq \emptyset$ for $1 \leq i < j \leq 3$ and $b_1 \cap b_2 \cap b_3 = \emptyset$, then $N_{\mathrm{h}} = 1$ and $N_{\mathrm{c}} = 3$, so $N_{\mathrm{h}} = 2N_{\mathrm{c}} - 5$. Furthermore, we may add a fourth, fifth, ... disc, where each added disc generates two new holes—as illustrated in Figure 5 in the case of five discs—whereby $N_{\mathrm{c}} = 3, 4, \dots$ and $N_{\mathrm{h}} = 2N_{\mathrm{c}} - 5$ in each case.

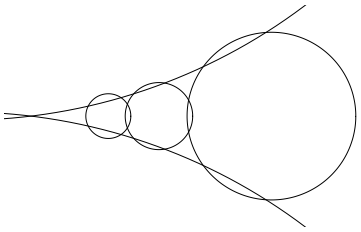

Figure 5. A configurations of five discs with exactly $2N_{\rm c}-5$ holes.

Kendall et al. [7] noticed the inclusion-exclusion formula for the functionals $W = A, L, \chi$:

$$W(\mathcal{U}_{\mathbf{x}}) = \sum_{1}^{n} W(b_i) - \sum_{1\le i<j\le n} W(b_i \cap b_j) + \cdots + (-1)^{n-1} W(b_1 \cap \cdots \cap b_n)$$

where the sums involve $2^n - 1$ terms. Using the power tessellation, inclusion-exclusion formulae with much fewer terms are given by (6)-(7) for χ and $N_{\rm bv}$, and by Proposition 2 below for A and L. In Proposition 2, $I_1(\mathbf{x})$, $I_2(\mathbf{x})$, and $I_3(\mathbf{x})$ denote index sets corresponding to non-empty cells, interior edges, and interior vertices of $\mathcal{B}_{\mathbf{x}}$, respectively. Note that $I_1(\mathbf{x})$ and $I_2(\mathbf{x})$ correspond to the cliques in the dual graph $\mathcal{D}_{\mathbf{x}}$ consisting of 1 and 2 nodes, respectively, while $I_3(\mathbf{x})$ corresponds to the subset of 3-cliques $\{i,j,k\} \in \mathcal{D}_{\mathbf{x}}$ with $b_i \cap b_j \cap b_k \neq \emptyset$ (i.e. $b_i \cup b_j \cup b_k$ has no hole). Moreover, if $\{i,j,k\} \in \mathcal{D}_{\mathbf{x}}$, then $b_i \cap b_j \cap b_k \neq \emptyset$ if and only if $E_{i,j} \cap E_{i,k} \neq \emptyset$, where the latter property is easily checked.

Proposition 2. The following inclusion-exclusion formulae hold for the area and perimeter of the union of discs:

$$A(\mathcal{U}_{\mathbf{x}}) = \sum_{i\in I_1(\mathbf{x})} A(b_i) - \sum_{\{i,j\}\in I_2(\mathbf{x})} A(b_i \cap b_j) + \sum_{\{i,j,k\}\in I_3(\mathbf{x})} A(b_i \cap b_j \cap b_k) \quad (12)$$

$$= \sum_{i\in I_1(\mathbf{x})} A(B_i) \quad (13)$$

and

$$L(\mathcal{U}_{\mathbf{x}}) = \sum_{i\in I_1(\mathbf{x})} L(b_i) - \sum_{\{i,j\}\in I_2(\mathbf{x})} L(b_i \cap b_j) + \sum_{\{i,j,k\}\in I_3(\mathbf{x})} L(b_i \cap b_j \cap b_k) \quad (14)$$

$$= \sum_{e \text{ boundary edge of } \mathcal{B}_{\mathbf{x}}} L(e). \quad (15)$$

Proof. Equations (12) and (14) are due to Theorem 6.2 in [4], while (13) and (15) follow immediately.

Edelsbrunner [4] establishes extensions to $\mathbb{R}^d$ of the inclusion-exclusion formulae given by the second identities in (6), (12), and (14). Note that we cannot replace the sums in (12) by sums over all discs, pairs of discs, and triplets of discs from $\mathbf{x}$.

6.2. Local calculations

For calculating the area and perimeter, the inclusion-exclusion formulae (13) and (15) appear to be more suited than (12) and (14) when the computations are done in combination with the sequential constructions of power tessellations considered in Section 4.2 and Section 5. Note that we need only to do "local computations".

For example, suppose we are given the power tessellation $\mathcal{B}^{\rm old}$ of $\mathcal{U}^{\rm old} = \cup_1^{n-1} b_i$ and add a new disc b_n. When constructing the new power tessellation $\mathcal{B}^{\rm new}$ of $\mathcal{U}^{\rm new} = \cup_1^{n} b_i$, we need only to consider the new set B_n and the old cells in $\mathcal{B}^{\rm old}$ which are neighbours to B_n with respect to the dual graph of $\mathcal{B}^{\rm new}$, cf. Section 5.1. Similarly, when a disc is deleted and the new tessellation is constructed, we need only local computations with respect to the discs intersecting the disc which is deleted, cf. Section 5.2. Moreover, local computations are only needed when calculating $N_{\rm ic}$ and $N_{\rm bv}$.

In order to calculate $(\chi, N_{\rm h})$ or equivalently $(N_{\rm cc}, N_{\rm h})$, we could keep track on the inner and outer boundary curves in our sequential constructions, using a clockwise and anticlockwise orientation for the two different types of boundary curves. However, in our MCMC simulation codes, we found it easier to keep track on $N_{\rm c}, N_{\rm ie}, N_{\rm iv}$, and $N_{\rm cc}$, and thereby obtain χ by the second equality in (7), and hence $N_{\rm h}$ by the first inequality in (7). In either case, this is another kind of local computation.

Finally, let us explain in more detail how we can find the area A. We can easily determine the total area of all isolated cells of $\mathcal{B}$. Suppose that B_i is a non-empty, non-isolated cell of $\mathcal{B}$. Let c_i denote the arithmetic average of the vertices of B_i. Then $c_i \in B_i$, since B_i is convex. For any three points $c, u, v \in \mathbb{R}^2$, let $\Delta(c,u,v)$ denote the triangle with vertices c, u, v. If $\lfloor u, v \rceil$ is a boundary edge of B_i, let $\Gamma(u,v)$ denote the cap of b_i bounded by the arc $\lfloor u, v \rceil$ and the line segment $[u,v]$. Then the area of B_i is the sum of areas of all triangles $\Delta(c_i,u,v)$, where u and v are defining an (interior or boundary) edge of B_i, plus the sum of areas of all caps $\Gamma(u,v)$, where u and v are defining a boundary edge of B_i.

7. Statistical aspects

As an illustrative application example, we consider the well known heather dataset first presented in Diggle [3]. Fig. 6 shows a binary image of the presence of heather (*Calluna vulgaris*, indicated by black) in a 10×20 m rectangular region W at Jädraås, Sweeden (henceforth units are meters). Assuming the heather plants grow from seedlings

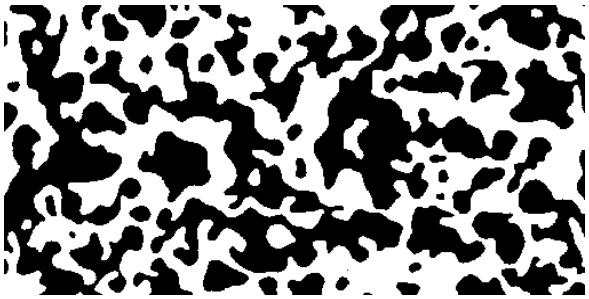

Figure 6. The heather dataset.

into roughly hemispherical bushes, a disc process model has a straightforward biological interpretation by identifying heather bushes and discs.

Edge effects occur, since the heather plants expand outside the observation window W, where W is a subset of S, the bounded region of plants centres. In fact S is unknown to us, but this problem and the problem of edge effects can be solved as discussed in detail in [12]; for the present paper it suffices to think of S as a much larger region than W.

Diggle [3] and many other publications modelled the presence of heather by a stationary random-disc Boolean model, see the review in [12]. For the reference Poisson process, let $\rho = 2.45$ be constant on S and Q be the uniform distribution on $[0, 0.53]$ (independent biological evidence suggests that the radii of heather plants should be less than 0.5 m, cf. [3]; (3); see also the discussion in [12]).

For the T-interaction process, let $\theta_5 = \theta_6 = 0$. This is mainly for convenience, since the number of isolated cells and the number of boundary vertices will be hard to determine from Fig. 6, the heather plants may only approximately be discs, and only a digital image is observed where the resolution makes it difficult to identify circular structures. As discussed in [12], the model can be reduced to the case where $\theta_3 = \theta_4$ so that $\theta = (\theta_1, \theta_2, \theta_3, \theta_3, 0, 0)$ and hence

$$f_\theta(\mathbf{x}) = \frac{1}{c_\theta} \exp\left(\theta_1 A(\mathcal{U}_\mathbf{x}) + \theta_2 L(\mathcal{U}_\mathbf{x}) + \theta_3 N_{\mathrm{cc}}(\mathcal{U}_\mathbf{x})\right), \tag{16}$$

i.e. the important characteristics are the area A, the perimeter L, and number of connected components N_{cc}. Approximate maximum likelihood estimates of the parameters are then given by $\hat{\theta}_1 = -4.91$, $\hat{\theta}_2 = 1.18$, and $\hat{\theta}_3 = 2.25$, and approximate 95% confidence intervals are given by $-6.48 \leq \theta_1 \leq -3.35$, $0.77 \leq \theta_2 \leq 1.59$, and $-2.75 \leq \theta_3 \leq -1.75$. For further details, including a discussion of other fitted models and model controls, see again [12].

Using simulations under the fitted model (16), we obtain an estimated intensity of plants given by 2.36 plants per unit area, and an estimated mean plant radius of 0.25 with an estimated standard deviation of 0.25. Further, Fig. 7 shows

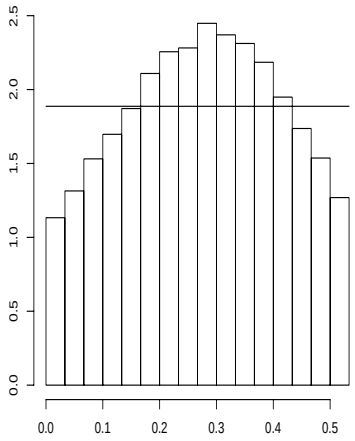

Figure 7. Estimated distribution of the plant radius under the fitted (A, L, N_{cc})-interaction process. The solid line show the uniform density of the typical radius under the corresponding reference Poisson process.

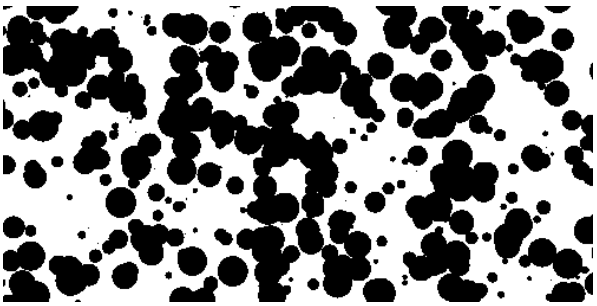

Figure 8. Simulation of the Boolean model corresponding to the reference Poisson process

the estimated distribution of the plant radius, which is obviously different from a uniform distribution. Furthermore, Fig. 8 shows a simulation under the the reference Poisson process, and Fig. 9 a simulation under the fitted (A, L, N_{cc})-interaction process. These figures together with other plots in [12] indicate that the T-interaction process provides a much better fit than the traditional Boolean model.

8. Concluding remarks

We have demonstrated the usefulness of the power tessellation of a union of discs and related results for geometric characteristics of this tessellation when simulating a disc process with a density which only depends on such characteristics. In this connection a successive construction of power tessellations when adding or removing a single disc has been developed, new interesting relations between the geometric characteristics have been established, and software have been developed and made public available.

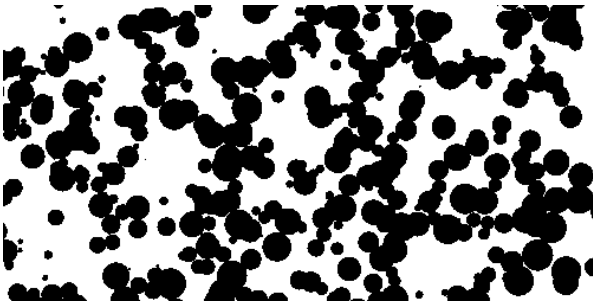

Figure 9. Simulation of the fitted (A, L, N_{cc})-interaction process.

As an application example, we have fitted our model to a heather dataset. Since the heather dataset are rather smooth while a disc process is naturally more rugged, possibly an even better fit may be obtained by replacing the disc process with a process of objects with a less restrictive form, e.g. obtained by considering random deformations of discs. To which extent the useful results discussed in this paper extend to the case of a process of objects with non-circular shapes is an open problem.

Acknowledgment

We are grateful to Lars Døvling Andersen, Herbert Edelsbrunner, and Wilfrid Kendall for useful comments, and to Adrian Baddeley for providing the dataset. Supported by the Danish Natural Science Research Council, grant 272-06-0442, "Point process modelling and statistical inference", and by grants from Czech Government reseach program MSM6840770038 and IAA101120604.

References

[1] F. Aurenhammer, "Power diagrams: properties, algorithms and applications," SIAM Journal on Computing, vol. 16, 1987, pp. 78-96.

[2] K. S. Chan and C. J. Geyer, "Discussion of the paper 'Markov chains for exploring posterior distributions' by Luke Tierney". Ann. Statist., vol. 22, 1994, p. 1747.

[3] P. J. Diggle, "Binary mosaics and the spatial pattern of heather," Biometrics, vol. 37, 1981, pp. 531-539.

[4] H. Edelsbrunner, "The union of balls and its dual shape," Discrete Comput. Geom., vol. 13, 1995, pp. 415-440.

[5] C. J. Geyer, "Likelihood inference for spatial point processes", in *Stochastic Geometry: Likelihood and Computation*. Eds. O. E. Barndorff-Nielsen, W. S. Kendall, and M. N. M. van Lieshout. Boca Raton, FL: Chapman & Hall/CRC, 1999, pp. 79-140.

[6] C. J. Geyer and J. Møller, "Simulation procedures and likelihood inference for spatial point processes". Scand. J. Statist., vol. 21, 1994, pp. 359-373.

[7] W. S. Kendall, M. N. M. van Lieshout, and A. J. Baddeley, "Quermass-interaction processes: Stability properties", Adv. Appl. Probab. vol. 31, 1999, pp. 315-342.

[8] W. S. Kendall and J. Møller, "Perfect simulation using dominating processes on ordered spaces, with application to locally stable point processes", Adv. Appl. Probab. vol. 32, 2000, pp. 844-865.

[9] I. Molchanov, *Statistics of the Boolean Model for Practitioners and Mathematicians*. Chichester, England: Wiley, 1997.

[10] J. Møller, *Lectures on Random Voronoi Tessellations*. Lecture Notes in Statistics 87. New York, NY: Springer-Verlag, 1994.

[11] J. Møller and K. Helisová, "Power diagrams and interaction processes for unions of discs," Adv. Appl. Probab. vol. 40, 2008, pp. 321-347.

[12] J. Møller and K. Helisová, "Likelihood inference for unions of interacting discs", Scand. J. Statist., in press.

[13] J. Møller and R. P. Waagepetersen, *Statistical Inference and Simulation for Spatial Point Processes*. Boca Raton, FL: Chapman and Hall/CRC, 2004.

[14] A. Okabe, B. Boots, K. Sugihara, and S. N.Chiu, *Spatial Tessellations. Concepts and Applications of Voronoi Diagrams*, second ed. Chichester, England: Wiley, 2000.

[15] G. O. Roberts and J. S. Rosenthal, "Geometric ergodicity and hybrid Markov chains". Electronic Communications in Probability, vol. 2, 1997 pp. 13-25.

[16] R. J. Wilson, *Introduction to Graph Theory*. Edinburgh, Scotland: Oliver and Boyd,1972.